Modeling of Brazing Processes That Use Coatings and Interlayers

Transport behavior of chemical elements at the braze interface is emphasized in the modeling of three coatings

BY S. LIU, D. L. OLSON, G. P. MARTIN AND G. R. EDWARDS

ABSTRACT. The possibility of using the new coating technologies in brazing is examined. By depositing one or more layers of filler metals on the joint surfaces, traditionally difficult-to-join materials can be brazed together. Barrier coatings, coatings for dissolution-solidification, and reactive metal coatings (interlayers) are the three different groups of coatings discussed. To control brazing, the optimal amount of coating applied must be determined and the interfacial chemical reactions must be understood, with the characterization of the products that result in the braze metal. Mathematical modeling of brazing using the three types of coatings is performed to describe the transport of chemical elements at the braze interface.

Introduction

The brazing of advanced engineering materials, and especially dissimilar materials, is coupled to the effective use of coatings. The most obvious application is to use the coating process to establish a highly wettable surface for the liquid filler metal. The coating may also be used as a barrier when the brazing filler metal is incompatible with the base material, to avoid diffusion of certain alloying elements and to prevent intermetallics formation.

Recent approaches (Ref. 1–3) to coating technology in brazing recognize that coatings are no longer just an intermediate passive barrier, but they take an active part in the brazing process. Mass transport, either from the brazing filler metal into the base material or the dissolution of the coating into the braze metal, can promote physical changes, such as increasing the liquidus temperature of the braze metal, which affect significantly the brazing process. With proper selection of the coating material and brazing filler metal, very consistent brazing processes can be developed. The control of the chemical composition and thickness of the coating layers are far more critical than that required in traditional brazing filler metals. This paper places emphasis on the existing coating technology applied in brazing and presents an analysis of the mass transport behavior of these advanced coating-brazing processes. With the proper understanding and knowledge of the behavior of these coatings, filler metals and processing conditions can be selected according to sound engineering principles. It is postulated that joining of difficult-to-join materials should be possible by applying multiple coatings, which create conditions such as wetting and chemical affinity between the faying surfaces.

S. LIU, D. L. OLSON, G. P. MARTIN and G. R. EDWARDS are with the Center for Welding and Joining Research, Colorado School of Mines, Golden, Colo.

Brazing Coating Technology

There are many ways to apply coatings on parts to be brazed. They are: 1) electrolytic: electroplating or electroless deposition; 2) thermal: dip coating, barrel coating, roller coating, flow melting, etc.; 3) surface modification: cladding, thermal spraying, plasma spraying, etc.; and 4) physicochemical: sputtering deposition, vapor deposition, ion implantation, etc. Since both chemical homogeneity and thickness are important properties of a coating, the coating procedure must be well controlled. For components that require critical dimensional control, continuous sputter-cleaning and vapor deposition-type processes are preferred because of the uniform adhesion obtained at the interfaces.

Three different coating schemes are described below, each serving a specific function in brazing. They are: 1) barrier coatings, 2) reactive metal coatings, and 3) coatings for dissolution-solidification.

KEY WORDS

Brazing Filler Metal
Brazing Coatings
Transient Liquidus Phase Modeling
Brazing Metallurgy
Filler Metal Selection

Barrier Coatings

It has been common practice, when no known suitable brazing filler metal is available for the materials to be joined, to use a coating that can be wetted by the liquid braze (Ref. 4). The coating also serves as a barrier between the base metal and the braze during processing. A barrier layer must be dense, ductile and free from defects such as voids. It must also show good adhesion and wetting toward both the base and filler metals. Copper-phosphorus filler metal had been used in the past to join ferrous alloys; however, intergranular penetration of phosphorus was observed to promote subsurface embrittlement of the joint. A thin undercoating of nickel reduced phosphorus diffusion and provided good wetting for the copper-phosphorus filler metal (Ref. 5). Similar techniques are used in soldering brasses. A 1- to 2-μm-thick layer of nickel or copper barrier coating is often used to avoid zinc diffusion to tin or tin-lead filler metals (Ref. 6). In electronic packaging, tin-lead alloys alone will not wet a ceramic substrate. A layer of silver or gold of adequate thickness is often deposited to provide a wettable surface for the tin-lead alloys (Ref. 4).

Sometimes the barrier coating scheme may require a double coating. Material for the first layer is selected for its compatibility with the base metal and the second layer (overlayer or outer coating) is used to promote wetting with the liquid brazing filler metals, as illustrated in Fig. 1. The primary layer is generally a transition metal solution containing polyvalent elements such as titanium, manganese, zirconium, tantalum, or molybdenum, where the polyvalent states increase the bonding tendency. The second layer is usually a thin layer of noble metal which provides a surface that is oxide-free, or with a very thin oxide layer which readily decomposes or dissolves during brazing. Such oxygen-free surfaces have, in general,

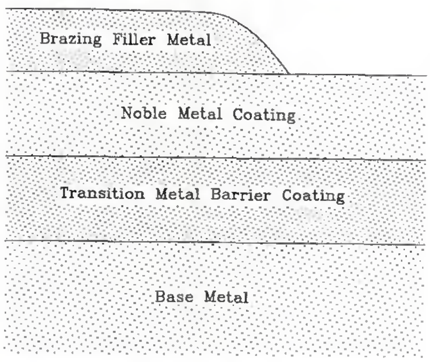

Fig. 1 — Schematic diagram showing the noble metal and transition metal barrier coatings inserted between the base metal and the brazing filler metal.

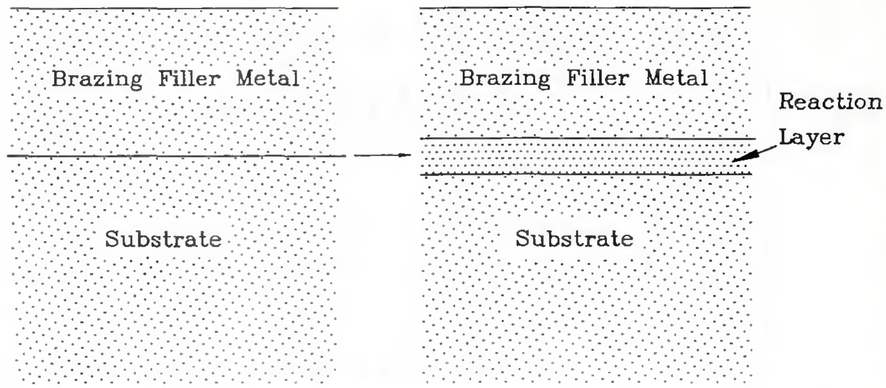

Fig. 2 — Schematic drawing showing the formation of a reaction layer between the substrate and brazing filler metal.

high surface energy and offer excellent wettability. Metals such as silver, gold and copper serve this function, requiring little, if any, fluxing agent. The double coating scheme will also allow for longer brazing times since the thickness of the outer coating can be adjusted to satisfy the needs of specific thermal processing cycles.

Reactive Metal Coatings

The use of reactive metals in brazing has been shown to promote the formation of a thin interlayer between the brazing filler metal and the base metal (Refs. 12–15). This layer promotes adhesion between the faying surfaces of similar and dissimilar materials. Hence, the resulting strength of the braze is dependent upon the nature of the product layer and its thickness. An example is the use of titanium in noble-metal-based brazing filler metals for the joining of metals to ceramic materials. Titanium in the liquid braze metal reacts with the substrate to form a thin reaction layer as shown in Fig. 2. This product layer can be a complex oxide such as Cu_2Ti_4O and $Cu_3Ti_3O_2$, or an intermetallic compound, depending whether the base material is an oxide ceramic or a metal. Certain types of complex oxide (for example, $(Cr,Mn,Mg)O.(Cr,Mn,Al)_2O_3$ spinel) also promote adhesion between metal and oxides as observed in the case of poor slag detachability in stainless steel welding (Ref. 16). The characterization and understanding of the crystal structure and microstructure of the product layers must be carried out so that adequate process control can be achieved.

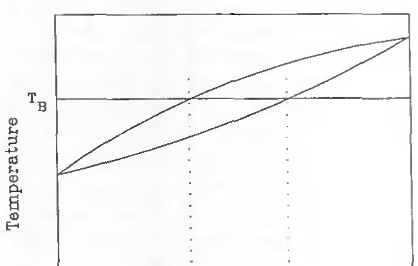

Fig. 3 — An isomorphous copper-nickel binary phase diagram showing the solidus and liquidus compositions at the brazing temperature, T_B.

The thickness of this layer will depend on the reaction kinetics, which is a function of the reactive metal content, diffusion of species through the product layer, brazing time and temperature. Brazed joints with inadequate product layer thickness, the result of improper brazing, may not meet the mechanical requirements specified for the joint. Hence, the use of reactive elements as brazing filler metal is a mass transport-based technology that must be investigated and understood.

Coatings for Dissolution-Solidification

Some coatings are deposited for the purpose of dissolution and solidification. In contrast to the passive barrier coatings, these dissolution-solidification coatings are considered active because of their contribution to the braze metal composition and its thickness. A good example is the transient liquid phase (TLP) bonding. TLP bonding is a diffusion brazing process that combines the features of both brazing and diffusion welding (Refs. 7–9). It uses as filler metal a thin interlayer or brazing filler metal of specific composition and melting temperature. At the bonding temperature, the interlayer may melt or a liquid may form by alloying between the interlayer metal and the base metal. The liquid, by capillary action, fills the joint clearance and contributes to the elimination of voids at the braze interface. While the joint members are held at the bonding temperature, diffusion of alloying elements occurs between the liquid and base metal. Isothermal solidification of the joint results because of the solute composition change in the braze. Maintaining the joint at the bonding temperature after solidification will promote further homogenization of the chemical composition and microstructure. Solid-state diffusion of elements away from the interfacial region reduces the initially large chemical composition gradient, avoiding the formation of intermetallics at the braze. An element of high mobility, both in the liquid and solidified braze metal, will decrease the time for completion of the TLP process.

As an example, consider the brazing of nickel (or a cupronickel alloy) with a pure copper filler metal of half-thickness, W_o. It can be seen in the phase diagram (Fig. 3) that when the temperature of the joint is raised to the brazing temperature T_B (T_B being greater than the melting point of copper), the copper melts and the solid nickel interface is enriched with copper, $X^s_{Cu}|_{T_B}$, which lowers its liquidus temperature to T_B (quasi-equilibration). Mass transfer of copper from the liquid phase proceeds to dissolve the nickel base metal and simultaneously enrich the liquid phase with nickel. This process continues until the liquid interphase composition, $X^l_{Cu}|_{T_B}$, becomes uniform throughout the liquid. Now, solid-state diffusion of nickel from the base metal will enrich the solid interphase region resulting in concomitant solidification (at a much slower rate than the previous base metal dissolution) under isothermal conditions. The liquid zone will eventually resolidify, and its composition will later become uniform, provided sufficient time is allowed for the solid-state diffusion process to occur. The events described above are depicted in Fig. 4.

Conventional transient liquid phase bonding is mostly applied to binary alloy systems which show some intermediate, low-temperature reactions such as eutectic transformation. However, by using an interlayer of adequate thickness that wets the base metal or barrier coating, alloy systems currently not considered for TLP bonding can also be joined by this method. Depending on the rate that the liquid braze dissolves the coating, the proper thickness of a suitable coating and the optimal brazing temperature can be determined, (Refs. 10–11).

An analytical model of the TLP bonding process with coating is developed and presented in a later section of this paper. The proposed approach can provide the basis for the selection of braze and coating materials and processing conditions.

Mathematical Modeling of Brazing Processes

It has been shown in the previous sections that with careful process control, coatings can be used effectively to braze difficult-to-join materials and produce bonds of high integrity. The need for process modeling to optimize joining parameters such as coating thickness, brazing time and temperature is also clear. This section will review the existing mathematical formulation of the mass transport processes involved in the brazing processes that utilize coatings.

Barrier Coatings

When using a double-layered barrier coating in brazing, the layer closest to the base metal (inner coating) is considered passive, and the outer or overlayer is active. The major function of the inner coating is to isolate the base metal from the brazing filler metal since this may contain chemical elements that are undesirable to the system. The passive coating is generally a high-melting-temperature metal and highly adherent to the base metal. It should exhibit excellent base metal wetting and remain solid throughout the brazing process. On the other hand, the overlayer should promote wetting with the brazing filler metal and dissolve entirely or partly into the braze during brazing. Metal dissolution is well characterized and modeled (Refs. 17–20) with extensive literature available. Therefore, no further mathematical modeling on brazing with a barrier coating will be presented in this paper.

Coatings for Dissolution-Solidification

In the case of a coating for dissolution and solidification, the composition of the coating must be carefully selected to be compatible with the brazing filler metal. The requirements for a brazing filler metal are illustrated in Fig. 5. The phase diagram is for a binary alloy, but this is not a necessary restriction since ternary brazing filler metals could also be considered. In Fig. 4, C_o^B is the initial brazing filler metal composition and B is the coating material. As B dissolves into the liquid braze metal at T_B, the liquid is continuously consumed to produce a solid of composition C_f^B, the final (new) composition of the solidified braze metal. The solidus of this new material has therefore been raised from T_1 to T_B.

Since brazing filler metals can be treated broadly as binary or ternary eutectic materials, there are specific ranges of braze metal compositions that can be used with a selected coating material. For example, consider the liquidus projection diagram in Fig. 6 where it is assumed that the three-phase triangles are traveling along the liquid projection lines according to a Class I, four-phase eutectic reaction (Ref. 21). Adjacent to each of these liquidus lines is a shaded zone which indicates compositions of potential brazing filler metals to be

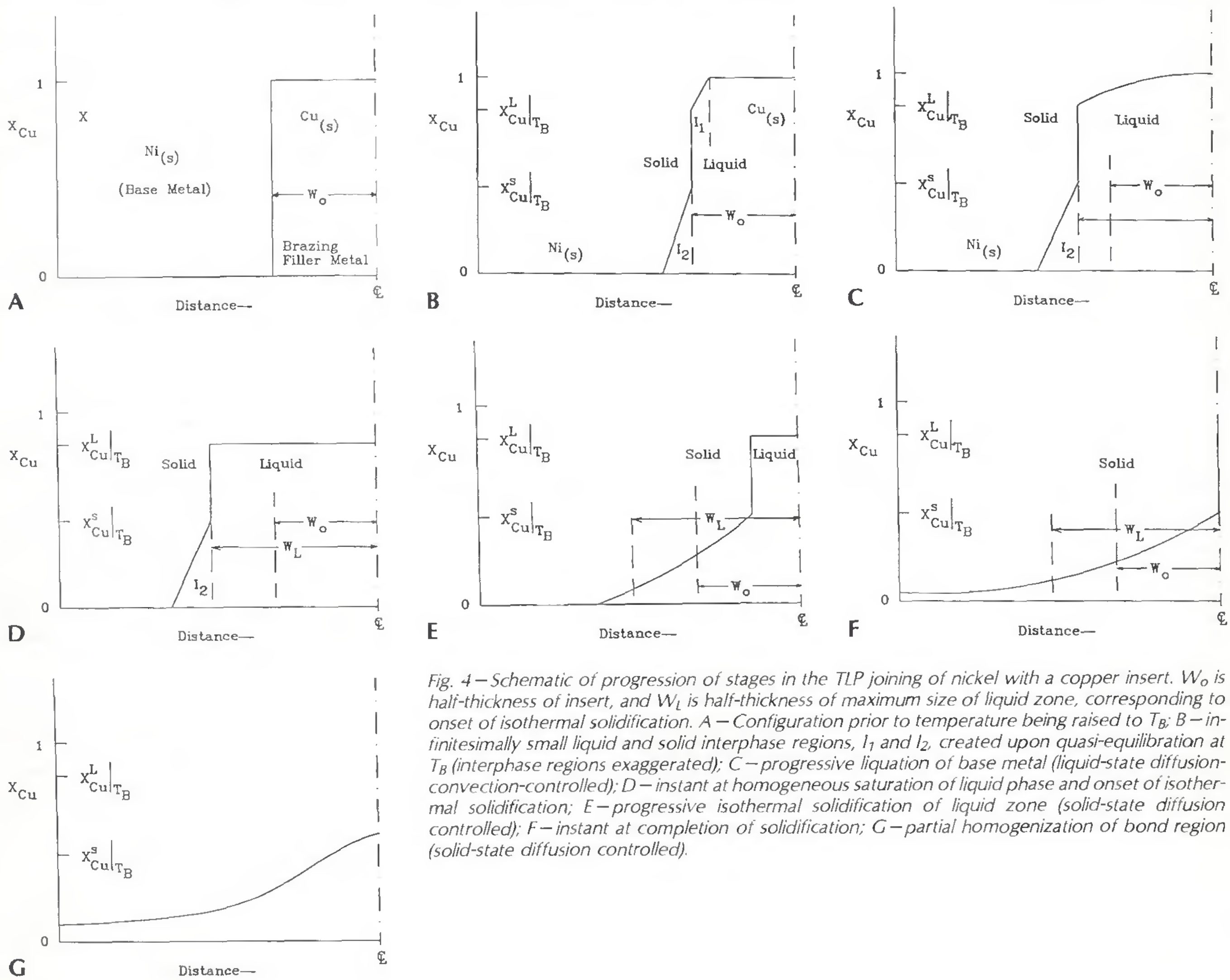

Fig. 4 — Schematic of progression of stages in the TLP joining of nickel with a copper insert. W_o is half-thickness of insert, and W_L is half-thickness of maximum size of liquid zone, corresponding to onset of isothermal solidification. A — Configuration prior to temperature being raised to T_B; B — infinitesimally small liquid and solid interphase regions, I_1 and I_2, created upon quasi-equilibration at T_B (interphase regions exaggerated); C — progressive liquation of base metal (liquid-state diffusion-convection-controlled); D — instant at homogeneous saturation of liquid phase and onset of isothermal solidification; E — progressive isothermal solidification of liquid zone (solid-state diffusion controlled); F — instant at completion of solidification; G — partial homogenization of bond region (solid-state diffusion controlled).

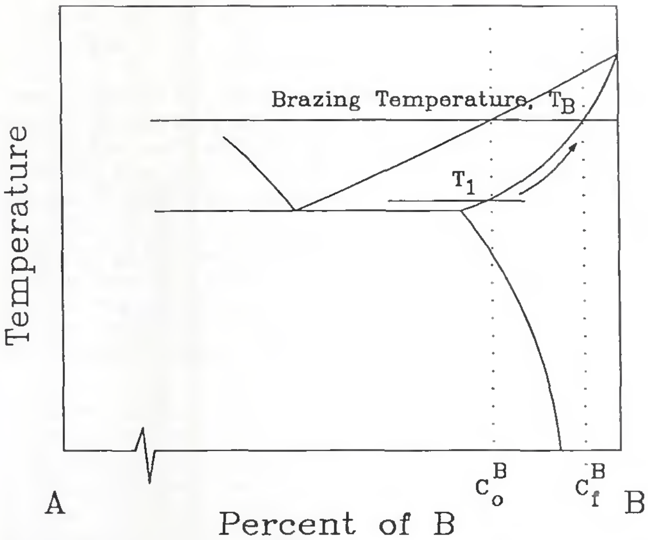

Fig. 5 — Partial binary phase diagram showing the compositions of the initial brazing filler metal, the coating, and the final braze metal composition at solidification.

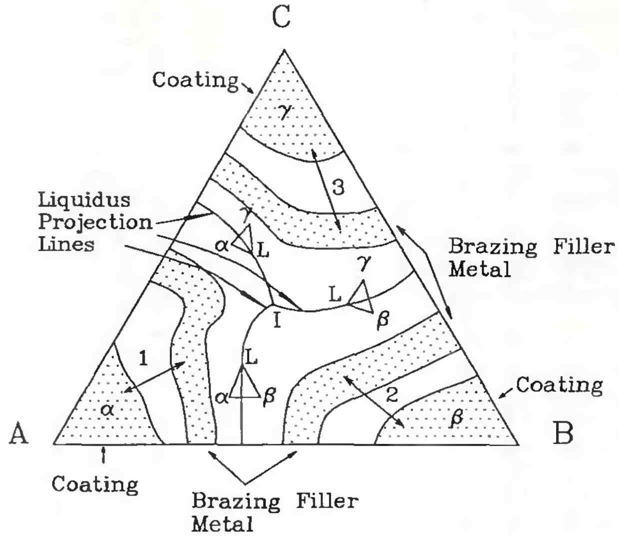

Fig. 6 — Ternary phase diagram indicating the different possible composition ranges of coating and brazing filler metal.

used, with their complementary coating materials. The coating materials are indicated in three separate alloy ranges, each adjacent to a brazing filler metal. The selection of brazing filler metal and complementary coating compositions are made for a given brazing temperature, and the time for which mutual dissolution will result in isothermal solidification. Phase equilibrium behavior illustrated in Fig. 6 can be found for some commonly used silver-iron-silicon filler metals (Ref. 10). Once the coating and brazing filler metals are identified, the resulting bond microstructure and properties will depend on the process temperature and time.

Lesoult (Ref. 22) modeled systematically the process of TLP bonding and divided the process into four stages: 1) dissolution of the interlayer; 2) homogenization of the liquid layer; 3) isothermal solidification; and 4) homogenization of the solidified braze metal. A binary system A-B was considered, and the equilibrium phase diagram is shown in Fig. 6. The brazing filler metals, with a B-component concentration, C_0^B (an alloy with a limited amount of A), was sandwiched between two substrates of composition, C_0. The dissolution and solidification stages were treated as a moving boundary problem involving a liquid and a solid, with local equilibrium at the solid-liquid interface. During dissolution, Fick's law was applied:

$$\frac{\partial C^L}{\partial t} = D_L\left(\frac{\partial^2 C^L}{\partial y^2}\right) \qquad (1)$$

where C^L is the concentration of the B component in the liquid of an A-B binary system, and y is the coordinate within the liquid region. Using the Error Function solution, the concentration profile that satisfies the above equation is given by:

$$C^L = E + F \operatorname{erf}\left(\frac{y}{\sqrt{4D_L t}}\right) \qquad (2)$$

where E and F are constants determined by the specific boundary conditions of the problem. D_L is the liquid diffusion coefficient of element B, and t is time. In addition, the interface displacement, Y_L, was constrained to obey the following square root law:

$$Y_L = K_L\sqrt{4D_L t} \qquad (3)$$

K_L was determined to be dependent on the particular alloy system and more specifically, on the slopes of the liquidus and solidus lines of the phase diagram. These lines influence the temperature dependency of the equilibrium concentrations at the liquid-solid phase boundaries.

Due to its complexity, the stage of homogenization of the liquid layer was not modeled (Ref. 22). During solidification, the displacement of the solid-liquid interface, at a particular brazing temperature, results from the solid-state diffusion of B to the saturated solid-liquid interface and can be expressed as:

$$Y_s = K_s\sqrt{4D_s t} \qquad (4)$$

and K_s in this equation can be obtained by solving the following implicit equation numerically:

$$K_s \exp(-K_s^2)(1 + \operatorname{erf} K_s)\sqrt{\pi} = \frac{(C^{\alpha L} - C_o)}{(C^{L\alpha} = C^{\alpha L})} \qquad (5)$$

$C^{L\alpha}$, $C^{\alpha L}$, and C_o are concentrations defined in Fig. 7, and appear in brackets to distinguish them from the notation used in the next section.

Similar to the dissolution case, K_s is dependent upon the properties of the materials system. Temperature will also influence K_s since the equilibrium concentrations $C^{L\alpha}$ and $C^{\alpha L}$ are temperature dependent.

Tuah-Poku, Dollar and Massalski (Ref. 23) investigated, more recently, the mechanisms of TLP bonding and developed further the earlier model by Lesoult (Ref. 22) and Sekerka (Ref. 24). In particular, they determined that the first stage of TLP bonding occurs almost instantaneously, with atomic diffusion taking place mainly in the liquid near the interlayer interface. The second stage is controlled by the diffusion of element B (component of the interlayer) in both the liquid and solid. The widening of the liquid zone was determined to follow a parabolic law.

Table 1—Values of the Growth Constants G^{α}_1 and G^{β}_1 for Dissolution of the Base Metal and Brazing Filler Metal for Typical Values of Λ_o and Λ_1

Λ_o	Λ_1	G^{α}_1	G^{β}_1
10	0.1	1.1513	0.3762
	0.2	0.9800	0.2416
	0.5	0.7502	0.1295
	1.0	0.5853	0.0819
	10.0	0.2095	0.0219
1	0.1	1.0597	1.0597
	0.2	0.8624	0.8624
	0.5	0.6201	0.6201
	1.0	0.4648	0.4648
	10.0	0.1568	0.1568
0.1	0.1	1.0395	1.7003
	0.2	0.8258	1.5372
	0.5	0.5529	1.3187
	1.0	0.3762	1.1513
	10.0	0.0819	0.5853

Modeling of TLP Brazing in This Work

In this study, the progressive stages of TLP bonding were reexamined and a different interpretation was developed. The major difference between this formulation and the models described in the previous section are the first two stages. In this approach, the dissolution of the interlayer and the widening of the liquid zone, as described by the previous models, are considered to occur simultaneously, followed by homogenization and solidification.

Examining the α-β couple shown in Fig. 8 (one-half of a braze joint), it is easy to realize that at high temperatures, atoms A will diffuse toward the β phase, and B atoms will diffuse toward the α phase. With the formation of the initial liquid zone, two solid-liquid interfaces are formed. Though at different rates, these interfaces will advance in opposite directions, consuming the α and β phases, respectively. With time, the brazing filler metal, β, will be totally consumed, to form one single liquid zone.

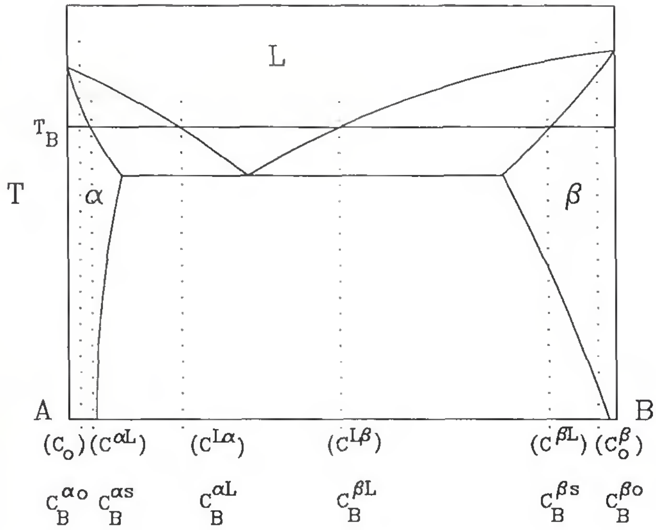

Fig. 7 — Binary phase diagram showing the composition of the different phases in TLP brazing.

Stage 1: Formation of the Liquid Zone

Referring to Fig. 8, in Stage 1, once the system is raised to the brazing temperature, T_B, the diffusion of element B in the quiescent liquid can be written as:

$$\frac{\partial C_B^L}{\partial t} = D_L \frac{\partial^2 C_B^L}{\partial y^2};\ Y_1^\alpha \geq y \geq -Y_1^\beta \tag{6}$$

with the following initial and boundary conditions:

$$\text{I.C. } C_B^L (y, t = 0)\text{: indeterminate} \tag{7}$$

$$\text{B.C.1 } C_B^L (y = -Y_1^\beta,\ t > 0) = C_B^{\beta L} \tag{8}$$

$$\text{B.C.2 } C_B^L (y = -Y_1^\alpha,\ t > 0) = C_B^{\alpha L} \tag{9}$$

Y_1^α and Y_1^β are the α-liquid braze metal and β-liquid braze metal interfaces, respectively. The compositions representing these boundary conditions can be seen in the binary phase diagram in Fig. 7. It should be noted that this notation is different from that used by Lesoult (Ref. 22), and also by Tuah-Poku, *et al.* (Ref. 23). The superscripts s and l have been used to identify the solid and liquid phases associated with the two solid solutions, α and β. The initial condition is indeterminate because the region where liquid exists is infinitesimally small. In regard to the equilibrium at the liquid-solid (α and β) interfaces, because of the infinitesimally small solid interface regions, they do not contribute to the mass balance in the system. Based upon the overall mass balance of component B in the solid phases (α and β) from which the liquid zone is created, the following equations for motion of the interfaces are determined:

$$\frac{dY_1^\alpha}{dt} = \frac{D_L}{C_B^{\alpha o} - C_B^{\alpha L}} \frac{\partial C_B^L}{\partial y} \Big|_{Y_1^\alpha} \tag{10}$$

and

$$\frac{dY_1^\beta}{dt} = \frac{-D_L}{C_B^{\beta o} - C_B^{\beta L}} \frac{\partial C_B^L}{\partial y} \Big|_{-Y_1^\beta} \tag{11}$$

Implicit in Equations 10 and 11 is that the partial molar volumes of all phases are equal (a restriction imposed on the solution presented here).

The initial conditions, provided that $C_B^{\alpha o}$ is less than $C_B^{\alpha s}$ and $C_B^{\beta o}$ is greater than $C_B^{\beta s}$, are:

$$Y_1^\alpha (t = 0) = Y_1^\beta (t = 0) = 0 \tag{12}$$

The solution to Equation 6 with the initial and boundary conditions represented by Equations 7–9 is:

$$C_B^L = U_1 + U_2 \operatorname{erf}\left(\frac{y}{2\sqrt{D_L t}}\right) \tag{13}$$

where U_1 and U_2 are constants that can be determined from the boundary conditions. Since the initial condition, as stated by Equation 7, is indeterminate, it does not impose a significant constraint on the behavior of the system as described by Equation 12.

The boundary conditions given by Equations 8 and 9 can be satisfied if:

$$C_B^{\beta L} = U_1 + U_2 \operatorname{erf}\left(\frac{-Y_1^\beta}{2\sqrt{D_L t}}\right) \tag{14}$$

and

$$C_B^{\alpha L} = U_1 + U_2 \operatorname{erf}\left(\frac{-Y_1^\alpha}{2\sqrt{D_L t}}\right) \tag{15}$$

Also, since U_1 and U_2 are constants, as well as the liquidus compositions $C_B^{L\beta}$ and $C_B^{L\alpha}$ (isothermal process), then the position of the solid-liquid interfaces can, therefore, only be described by:

$$Y_1^\alpha = 2G_1^\alpha \sqrt{D_L t} \tag{16}$$

and

$$Y_1^\beta = 2G_1^\beta \sqrt{D_L t} \tag{17}$$

where G_1^α and G_1^β are the dimensionless growth constants associated with each interface. It should be noted that the initial conditions indicated by Equation 12 are also satisfied by Equations 16 and 17.

Equations 14 and 15 can therefore be rewritten as:

$$C_B^{\beta L} = U_1 - U_2 \operatorname{erf}(G_1^\beta) \tag{18}$$

and

$$C_B^{\alpha L} = U_1 + U_2 \operatorname{erf}(G_1^\alpha) \tag{19}$$

On subtracting Equation 18 from 19 and rearranging, the following equation is obtained to determine U_2:

$$U_2 = \frac{C_B^{\alpha L} - C_B^{\beta L}}{\operatorname{erf}(G_1^\beta) + \operatorname{erf}(G_1^\alpha)} \tag{20}$$

Equations 16 and 17 can now be used to develop equations from which the growth constants G_1^α and G_1^β may be obtained. Differentiating these equations with respect to time gives:

$$\frac{dY_1^\alpha}{dt} = \frac{G_1^\alpha \sqrt{D_L}}{\sqrt{t}} \tag{21}$$

$$\frac{dY_1^\beta}{dt} = \frac{G_1^\beta \sqrt{D_L}}{\sqrt{t}} \tag{22}$$

Now, differentiating Equation 15 with respect to y, yields:

$$\frac{\partial C_B^L}{\partial y} = U_2 \frac{2}{\sqrt{\pi}} \exp\left(-\frac{y^2}{4D_L t}\right) \frac{1}{2\sqrt{D_L t}} \tag{23}$$

which, when evaluated at $y = Y_1^\alpha$ and $y = -Y_1^\beta$, leads to:

$$\frac{\partial C_B^L}{\partial y} \Big|_{y = Y_1^\alpha} = U_2 \frac{2}{\sqrt{\pi}} \exp(-G_1^{\alpha 2}) \frac{1}{2\sqrt{D_L t}} \tag{24}$$

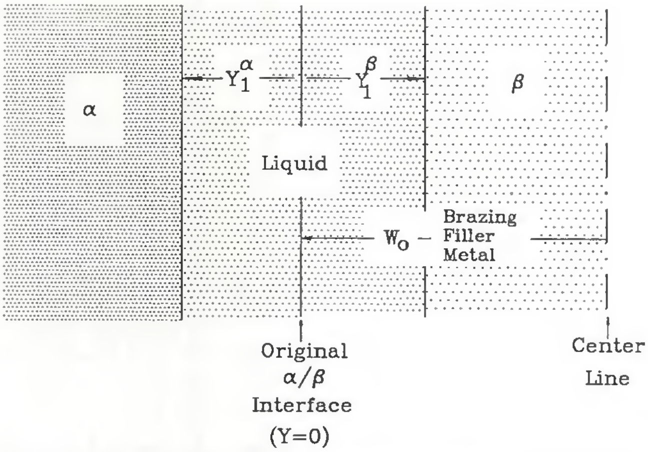

Fig. 8 — Configuration of α-phase base material, liquid region and β-phase brazing filler metal during isothermal liquification of solid phases, at time, t, after system is raised to brazing temperature, T_B.

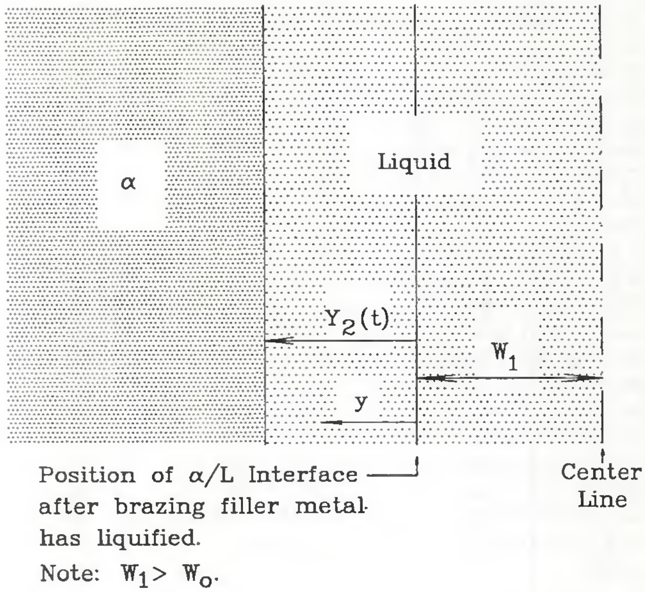

Fig. 9 — Configuration of system, at time, t, after brazing filler metal, of half-thickness, Wo, has liquified and liquid region becomes homogenized due to further dissolution of α-phase base metal.

$$\frac{\partial C_B^L}{\partial y}\bigg|_{y=Y_1^\beta} = U_2\frac{2}{\sqrt{\pi}}\exp\left(-G_1^{\beta 2}\right)\frac{1}{2\sqrt{D_L t}} \tag{25}$$

Substituting Equations 21, 22, 24 and 25 appropriately into Equations 10 and 11, the following equation is obtained when these two recast equations are divided, one by the other:

$$\frac{G_1^\alpha}{G_1^\beta} = \frac{C_B^{\beta o} - C_B^{\beta L}}{C_B^{\alpha L} - C_B^{\alpha o}}\exp\left(G_1^{\beta 2} - G_1^{\alpha 2}\right) \tag{26A}$$

Also, when Equation 20 is used to replace U_2 in Equation 24 and this is then substituted into the right-side of Equation 10, while the left side is replaced using Equation 21, the following additional equation is obtained:

$$G_1^\alpha = \frac{C_B^{\alpha L} - C_B^{\beta L}}{\mathrm{erf}(G_1^\beta) + \mathrm{erf}(G_1^\alpha)}\frac{1}{\sqrt{\pi}}\frac{\exp(-G_1^{\alpha 2})}{C_B^{\alpha o} - C_B^{\alpha L}} \tag{27A}$$

Equations 26A and 27A can be rewritten as follows:

$$\Lambda_o G_1^\beta \exp\left(G_1^{\beta 2} - G_1^{\alpha 2}\right) - G_1^\alpha = 0 \tag{26B}$$

$$\Lambda_1 G_1^\alpha \sqrt{\pi}\left[\mathrm{erf}(G_1^\beta) - \mathrm{erf}(G_1^\alpha)\right] - \exp\left(-G_1^{\alpha 2}\right) = 0 \tag{27B}$$

where

$$\Lambda_o = \frac{C_B^{\beta o} - C_B^{\beta L}}{C_B^{\alpha L} - C_B^{\alpha o}} \tag{28}$$

$$\Lambda_1 = \frac{C_B^{\alpha o} - C_B^{\alpha L}}{C_B^{\alpha L} - C_B^{\beta L}} \tag{29}$$

and it is noted that Λ_o and Λ_1 are both positive quantities. These stimultaneous equations, 26B and 27B, can be solved numerically to obtain the growth constants G_1^α and G_1^β once Λ_o and Λ_1 have been defined. Values of the growth constants are tabulated in Table 1. It should be noted that the physical behavior associated with the system is properly manifested by the values of the growth constants. For example, when Λ_o is unity, the growth constants are identical in magnitude. This is to be expected, since the enrichment of the liquid B provided via the β-phase filler metal is exactly compensated by the dilution due to the same volume of the α-phase base metal being consumed. Furthermore, when Λ_o is greater than unity the growth constant G_1^α is greater than G_1^β, as a result of a larger volume of the α- phase being required to compensate for the β-phase as the transient liquid is formed. The situation is reversed when Λ_o is fractional.

The formulation and solution presented here is significantly different from that presented by Tuah-Poku, Dollar and Massalski (Ref. 23) and attributed to Lesoult (Ref. 22), where only the growth constant for the liquid braze metal zone was considered.

The time at which a brazing filler metal of initial half-width, W_o, is consumed is given by:

$$t_1 = \frac{W_o^2}{4\,G_1^{\beta 2} D_L} \tag{30}$$

Also, the half-width of the liquid zone at this instant (prior to homogenization of the liquid), W_L, is given by:

$$W_L = W_o + 2\,G_1^\alpha\sqrt{D_L t_1} \tag{31}$$

Therefore, given the brazing temperature, metal compositions and interlayer thickness, then the time for interlayer dissolution, t_1, and the liquid zone half-width developed, W_L, can be calculated.

Stage 2: Homogenization of the Liquid Zone

During homogenization, Stage 2, the diffusion of B in the liquid phase is again described by:

$$\frac{\partial C_B^L}{\partial t} = D_L\frac{\partial^2 C_B^L}{\partial y^2};\ Y_2(t) > y > -W_1 \tag{32}$$

where now, only one moving boundary is present. The configuration at time, t, after this stage has started, is shown in Fig. 9. The initial condition is:

$$C_B^L(0 > y \geq -W_1,\ t = 0) = F(y) \tag{33}$$

where:

$$F(y) = C_B^{\beta L} + (C_B^{\alpha L} - C_B^{\beta L})\,\frac{\left[\mathrm{erf}(G_1^\beta) + \mathrm{erf}\left(G_1^\alpha + \frac{y}{\sqrt{2D_{Lt_1}}}\right)\right]}{\mathrm{erf}\,(G_1^\beta) + \mathrm{erf}\,(\Lambda_o G_1^\beta)} \tag{34}$$

$$W_1 = W_o + 2G_1^\alpha\sqrt{D_L t_1} = 2\sqrt{D_L t_1}\,(G_1^\alpha + G_1^\beta) \tag{35}$$

since W_o can be replaced using Equation 30.

The initial condition, Equation 34, describes the concentration profile in the liquid at the end of Stage 1. The boundary conditions are:

$$C_\beta^L\ [y = Y_2(t), t > 0] = C_B^{\alpha L} \quad (36)$$

$$\frac{\partial C_\beta^L}{\partial y}\Big|_{y=-W_{1,t}} = 0 \quad (37)$$

$$\frac{dY_2}{dt} = \frac{-D_L \frac{\partial C_L^B}{\partial y}\Big|_{Y_2(t)}}{(C_B^{\alpha L} - C_B^{\alpha o})} \quad (38)$$

with initial condition,

$$Y_2(t = 0) = 0 \quad (39)$$

A solution to Equation 32, with the initial and boundary conditions, and the moving boundary condition, most likely, will have to be determined numerically. While it is recognized that the time to complete Stages 1 and 2 of the process is small compared to that for Stage 3, nevertheless the maximum half-width, W_{max}, attained by the liquid zone is an inherent requirement for determining the time, t_3, for the isothermal solidification of the induced liquid zone.

The maximum half-width of the liquid zone can be calculated from mass balance constraints. For conservation of the component B:

$$W_{max}\ C_B^{\alpha L} = W_o C_B^{\beta o} + (W_{max} - W_o)\ C_B^{\alpha o} \quad (40)$$

or

$$W_{max} = \frac{C_B^{\beta o} - C_B^{\alpha o}}{C_B^{\alpha L} - C_B^{\alpha o}} W_o \quad (41)$$

Stage 3: Isothermal Solidification

Stage 3 is the isothermal solidification of the induced liquid zone. The configuration at some instant, t, after solidification has started is shown in Fig. 10. Diffusion of B in the solid α-phase can be described by the following equation:

$$\frac{\partial C_B^\alpha}{\partial t} = D_s \frac{\partial^2 C_B^\alpha}{\partial y^2};\ \infty \geq y \geq -Y_3 \quad (42)$$

The initial and boundary conditions are:

$$\text{I.C. } C_B^\alpha(y, t = 0) = C_B^{\alpha o} \quad (43)$$

$$\text{B.C.1 } C_B^\alpha(y = -Y_3, t > 0) = C_B^{\alpha s} \quad (44)$$

$$\text{B.C.2 } C_B^\alpha(y \rightarrow \infty, t) = C_B^{\alpha o} \quad (45)$$

The equation for motion of interface is:

$$\frac{dY_3}{dt} = \frac{-D_s}{C_B^{\alpha L} - C_B^{\alpha s}} \frac{\partial C_B^\alpha}{\partial y}\Big|_{y=-Y_3} \quad (46)$$

with initial condition:

$$Y_3(t = 0) = 0 \quad (47)$$

Note that $C_B^{\alpha o} < C_B^{\alpha s}$ and consequently component B diffuses into the solid base metal, thereby depleting the liquid of B and leading to its isothermal solidification. Equation 42 is satisfied by:

$$C_\beta^\alpha = U_1 + U_2\ \text{erf}\left(\frac{y}{2\sqrt{D_s t}}\right) \quad (48)$$

and the initial condition (Equation 43) and boundary condition (Equation 45) require that:

$$C_B^{\alpha o} = U_1 + U_2 \quad (49)$$

Also, the boundary condition given by Equation 44 can only be satisfied if:

$$C_B^{\alpha s} = U_1 + U_2\ \text{erf}\left(\frac{-Y_3}{2\sqrt{D_s t}}\right) \quad (50)$$

Furthermore, since U_1 and U_2 are constants, as well as the solidus composition, $C_B^{\alpha s}$ in the α phase during isothermal solidification, therefore the argument of the error function must also be a constant; consequently the position of the solid-liquid interface can only be described by:

$$Y_3 = 2\ G_3\sqrt{D_s t} \quad (51)$$

where G_3 is a dimensionless growth constant; and the initial condition as described by Equation 47 is satisfied by Equation 51. Consequently, since erf $(-x) = -$ erf (x), Equation 50 can be rewritten as:

$$C_B^{\alpha s} = U_1 - U_2\ \text{erf}(G_3) \quad (52)$$

Also, a general expression for the concentration gradient is obtained by differentiating Equation 48, with respect to y:

$$\frac{\partial C_B^\alpha}{\partial y} = U_2 \frac{2}{\sqrt{\pi}} \exp\left(\frac{-y^2}{4D_s t}\right) \frac{1}{2\sqrt{D_s t}} \quad (53)$$

Subtracting Equation 52 from Equation 49 gives the following expression for U_2:

$$U_2 = \frac{(C_B^{\alpha o} - C_B^{\alpha s})}{1 + \text{erf}\ (G_3)} \quad (54)$$

Finally, Equation 51 can be differentiated to obtain the velocity of the interface, *viz:*

$$\frac{dY_3}{dt} = G_3 \frac{\sqrt{D_s}}{\sqrt{t}} \quad (55)$$

Now, Equation 54 can be used to replace U_2 in Equation 53, and this expression together with Equation 55 to replace the respective terms in Equation 46, the following implicit equation for G_3 is obtained:

$$G_3\ [1 + \text{erf}\ (G_3)]\ \sqrt{\pi} \exp (-G_3^2) = \frac{C_B^{\alpha s} - C_B^{\alpha o}}{C_B^{\alpha L} - C_B^{\alpha s}} \quad (56)$$

which is identical to the equation attributed to Lesoult according to Tuah-Poku, Dollar and Massalski (Ref. 23).

If the maximum half-width of the induced liquid zone is W_{max}, then the elapsed time to complete the isothermal solidification is given by Equation 57, below:

$$t_3 = \frac{W_{max}^2}{4\ G_3^2\ D_s} \quad (57)$$

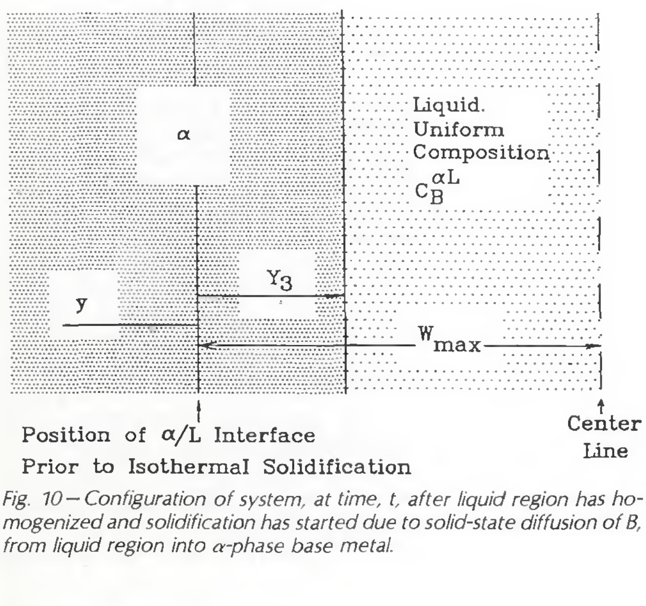

Fig. 10 — Configuration of system, at time, t, after liquid region has homogenized and solidification has started due to solid-state diffusion of B, from liquid region into α-phase base metal.

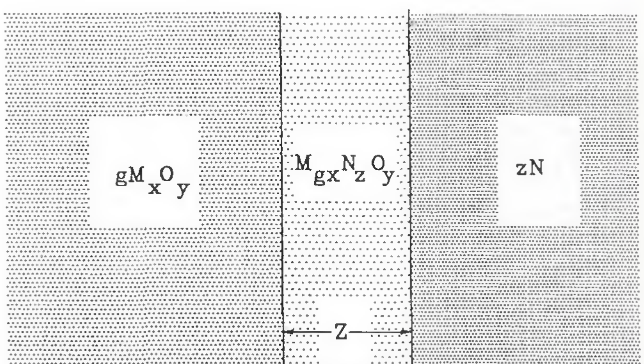

Fig. 11 — Schematic diagram showing the formation of a complex oxide layer in the joining of metals to ceramic materials.

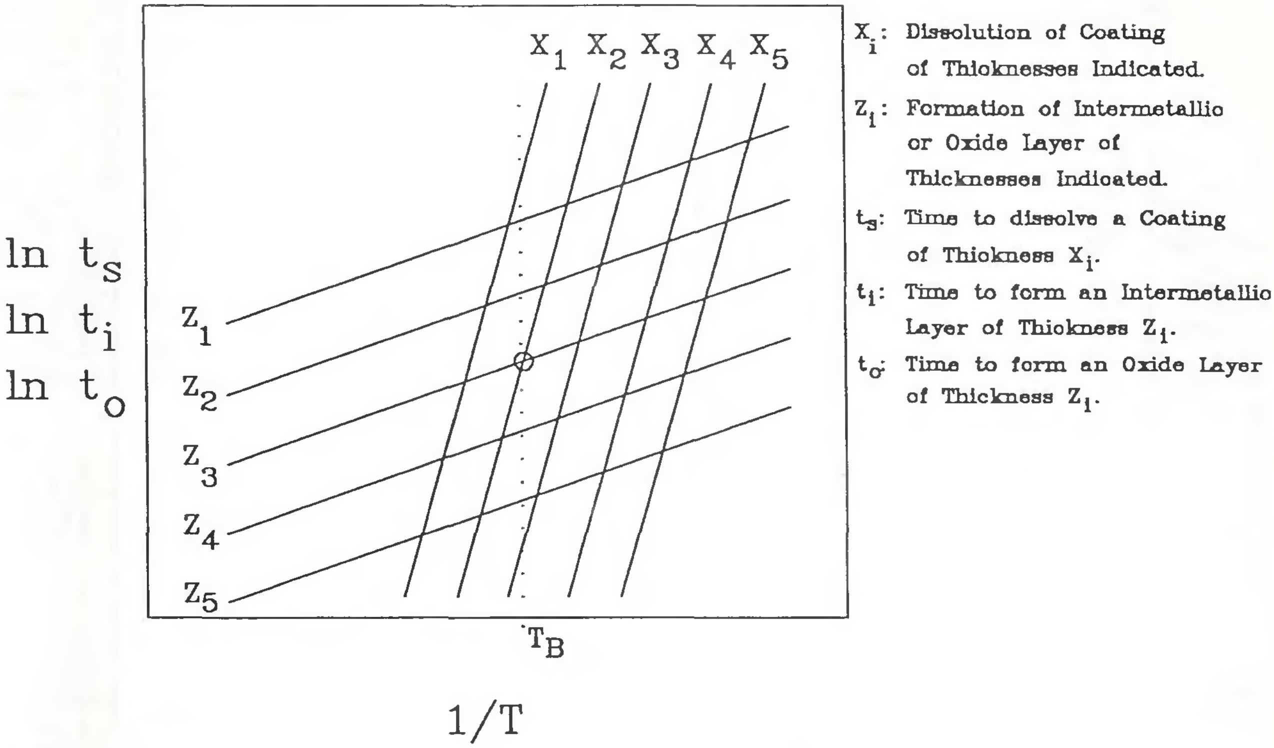

Fig. 12 — Conceptual brazing process control as a function of the time of dissolution of the coating, the time of oxide and intermetallic formation, and the brazing temperature. For an acceptable oxide layer thickness, Z_3, and maximum tolerable coating dissolution thickness, X_2, the brazing temperature should be T_B as indicated on the diagram.

where G is determined by solving Equation 56 numerically, for a given $C^{\alpha o}_{B}$, $C^{\alpha s}_{B}$, and $C^{\alpha l}_{B}$.

Modeling of Reactive Metal Brazing in This Work

There are numerous possible rate-controlling steps in this process. If the brazing filler metal has a very dilute reactive metal addition, the rate-controlling process may be the transport of the reactive element in the liquid braze to the reaction interface. One possible mass transport controlled process would be liquid diffusion where the reactive metal is consumed at the interface in product formation. However, a more realistic situation is where the product film or reaction layer is adhesive to and protective of the base metal, then solid-state diffusion across the interlayer will be the controlling process. A simple mathematical description for this moving boundary problem is given below. It is assumed that the chemical potentials are invariant at both interfaces and the layer thickness increases with time.

Depending on the base material to be joined — ceramic oxide or metal — the reaction product will be specific to that system. In metal-to-ceramic joining, it is most likely that an oxide layer will form. In the case of a metal, the equilibrium phase diagram determines whether a solid solution or intermetallic phase will form. The case of oxide formation is chosen to illustrate the procedure of determining the processing time, temperature and thickness of the coating to achieve an acceptable brazement. From the boundary condition described above, a parabolic time dependent growth of the product layer results. Figure 11 illustrates this oxide formation case.

Given the following reaction of oxidation:

$$zN + gM_xO_y \rightarrow M_{gx}N_zO_{gy} \tag{58}$$

and rate expression for growth of the product phase is given by:

$$Z^2 = 2K't \tag{59}$$

with:

$$K' = K_o \exp\left(\frac{-Q}{RT}\right) \tag{60}$$

where K′ is the rate coefficient, K_o is the preexponential factor, Z is the thickness of the product layer, and RT has the usual significance. The time to form a reaction layer of thickness Z can be determined by solving Equations 59 and 60.

$$\ln\ t_o = \ln\left(\frac{Z^2}{2K_o}\right) - \frac{Q}{RT} \tag{61}$$

where Q is the activation energy of the process and R is the universal gas constant. In the case of intermetallic formation, a similar equation will result.

Equation 61 is an important analytical tool in controlling reactive metal brazing. Too thin a reaction layer may not result in a sound braze while too thick a layer will result in excessive oxide/intermetallic compound growth and poor mechanical properties. Therefore, an optimal reaction layer thickness can be controlled by regulating process temperature and time.

Conceptual Application of Modeling to Process Control

In brazing, temperature, time and filler metal are some of the more important process parameters to be controlled and optimized. When a coating is introduced between the base material and brazing filler metal, active dissolution may occur at the interface between the brazing filler metal and the coating material. At the same time, chemical reactions may also occur at the base metal-coating interface. Since the kinetics of the two processes are in general not the same, it is essential to determine a set of optimal time and temperature for these simultaneous processes. It is obvious that the dissolution process should not consume the entire layer of coating, nor the intermetallic formation create an excessively thick product layer. To match the effects of interlayer dissolution and subsequent consumption of the coating with the formation of the oxide (or intermetallic) layer, the time for dissolution of selected coating thicknesses, X_1, X_2, . . ., X_5, can be plotted as a function of temperature. Increasing the temperature decreases the time of dissolution. The time of oxide (or intermetallic) formation and growth to selected thicknesses, $Z_1, Z_2, \ldots, Z_5$, can also be plotted likewise on the same figure. The two sets of parallel lines can be observed in Fig. 12. Since the thermally activated mechanisms of the two processes are different, the slope of the second set of lines is also different from that of the first set. For the oxide (or intermetallic) formation lines, the slope, associated with the parabolic growth law, is equal to Q/R; where Q is the activation energy of the transport mechanism of the growth process. Given a certain constraint of thickness of the oxide (or intermetallic) layer, then, the thickness of a coating that will be completely consumed by dissolution as well as the time and corresponding temperature of brazing can be determined from Fig. 12.

To illustrate the concept, consider the case where the oxide product layer must be limited to a thickness, Z_3 and an acceptable brazing time can be achieved at a temperature of T_1, the diagram indicates that the coating will be dissolved and be penetrated to a distance X_2 by the transient liquid phase bonding process. Consequently, the coating thickness selected must be larger than X_2.

In Fig. 12, the slope of the X lines (dissolution of the coating layer) is assumed to be greater than that of the oxide or intermetallic formation, Z lines. In the case that the slopes of both are changed, Z lines with greater slope than X lines, the interpretation procedure can still be followed.

Summary

It is apparent that coating technology, in particular the type for dissolution and solidification, can be applied in brazing. Multiple-layered coatings of different compositions can be tailored for difficult-to-join materials. With the mathematical models developed in this work, it is possible to begin addressing the design issues of brazing with custom coatings: types of coating, thickness of each layer, brazing time and temperature. Depending on the degree of dissolution of the coating and brazing filler metal, and the type of products that form at the base metal-coating and coating-brazing filler metal interfaces, the approach developed in this work will provide the basis for selecting brazing time, temperature and thickness of the coating for successful brazing.

Acknowledgment

The authors acknowledge and appreciate the support of the Office of Naval Research.

References

1. Funamoto, T., Kokura, S., Kato, M., Shida, T., and Oshima, K. 1985. A study on formation of alloyed layer of low melting temperature on bonding surface of IN 738 LC with sputtering. *Quarterly Journal of the Japan Welding Society,* 3(4):207-212.

2. Kato, M., Funamoto, T., and Wachi, H., Matsuzaka, T., Shida, T., and Kokura, S. 1987. A study of alloyed layer of low melting temperature on bonding surface of IN 738 LC with boron pack cementation. *Quarterly Journal of the Japan Welding Society,* 5(3):84-87.

3. Funamoto, T., Kato, M., Wachi, H., Kokura, S., Shida, T., and Matsuzaka, T. 1987. Diffusion weldability of IN 738 LC with alloyed layer on bonding surface by boron pack cementation. *Quarterly Journal of the Japan Welding Society,* 5(3):87-93.

4. Klein Wassink, R.J. 1984. Coated materials. *Soldering in Electronics,* 177-180, Electrochemical Publications Limited.

5. AWS. 1976. *Brazing Manual,* American Welding Society, Miami, Fla.

6. Bratton, S. C., and Clarke, M. 1959. Detection of zinc diffusion into tin coatings on brass. *Trans. Inst. Metal Finish.,* 36:230-232.

7. AWS. 1980. Diffusion welding and brazing. *Welding Handbook*-Vol. 3, 7th Edition, pp. 311-336, American Welding Society Miami, Fla.

8. Paulonis, D. F., Duvall, D. S., and Owczarski, W. A. 1972. *U.S. Patent 3,67B,570.*

9. Duvall, D. S., Owczarski, W. A., and Paulonis, D. F. 1974. T.L.P.: a new method for joining heat-resisting alloy. *Welding Journal,* 53(4):203-214.

10. Lammel, J. M., and Chalmers, B. 1959. The isothermal transfer from solid to liquid in metal systems. *Trans. TMS-AIME,* 215:499-508.

11. Bredzs, N., and Schwartzbart, H. 1959. Metallurgy of bonding in brazed joints. *Welding Journal,* 38:305-s to 314-s.

12. Tressler, R. E., Moore, T. L., and Crane, R. L. 1973. Reactivity and interface characteristics of titanium-alumina composites. *Journal of Materials Science,* 8:151-161.

13. Nicholas, M. G., Valentine, T. M., and Waite, M. I. 1980. The wetting of alumina by copper alloyed with titanium and other elements. *Journal of Materials Science,* 15:2197-2206.

14. Nicholas, M. G. 1986. Active metal brazing. *Trans. and Journal of the British Ceramic Society,* 85:144-146.

15. Nicholas, M. G., and Mortimer, D. A. 1985. Ceramic/metal joining for structural applications. *Materials Science and Technology,* 1:657-665.

16. Pincus, A. G. 1954. *Ceramic Age* 63:16,20, 30-33.

17. Tanzilli, R. A., and Heckel, R. W., 1968. Numerical solutions to the finite, diffusion-controlled, two phase, moving-interface problem (with planar, cylindrical, and spherical interfaces). *Trans. TMS-AIME,* 242:2313-2321.

18. Ohno, R. 1986. Rates of dissolution of solid iron, cobalt, nickel, and silicon in liquid copper and diffusion rate of iron from liquid Cu-Fe alloy into liquid copper. *Met. Trans. B,* 17:291-305.

19. Ishida, T. 1986. Rate of dissolution of solid nickel in liquid tin under static conditions. *Met. Trans. B,* 17:281-289.

20. Nakao, Y., Nishimoto, K., Shinozaki, K., Yun, K. C., and Hori, Y. Dissolution phenomenon of base metal into liquid insert metal. *Quarterly Journal of the Japan Welding Society,* 6(4):519-526.

21. Rhines, F. N. 1956. *Phase Diagrams in Metallurgy — Their Development and Application,* McGraw Hill Publishing Co.

22. Lesoult, G. 1976. Modeling of the TLP Bonding Process I. Report of the Center for the Joining of Materials, Carnegie-Mellon University.

23. Tuah-Poku, I., Dollars, M., and Massalski, T. B. 1988. A study of the transient liquid phase bonding process applied to a Ag/Cu/Ag sandwich joint. *Met. Trans. A,* 19:675-686.

24. Sekerka, R. F. 1980. On the modeling of TLP bonding. *Proc. of Physical Metallurgy of Metals Joining Conf.,* TMS-AIME, St. Louis, Mo.

Appendix

C_B^L	Concentration of B, in the (binary) liquid phase.
C_B^α	Concentration of B, in the α-phase (base metal) solid solution.
$C_B^{\alpha o}$	Initial (uniform) concentration of B in the α-phase.
$C_B^{\beta o}$	Initial (uniform) concentration of B in the β-phase.
$C_B^{\alpha s}$	Solidus concentration of B in the saturated α solid solution, at the isothermal solidification (brazing) temperature, T_B.
$C_B^{\beta s}$	Solidus concentration of B in the saturated β solid solution, at the isothermal solidification (brazing) temperature, T_B.
$C_B^{\alpha L}$	Liquidus concentration of B which is in equilibrium with the saturated α solid solution, of composition $C_B^{\alpha s}$
$C_B^{\beta L}$	Liquidus concentration of B which is in equilibrium with the saturated β solid solution, of composition $C_B^{\beta s}$
G_1^α	Growth constant for liquification of base metal, during Stage 1.
G_1^β	Growth constant for liquification of brazing filler metal, during Stage 1.
G_2	Growth constant for liquification of base metal, during homogenization of liquid region — Stage 2.
G_3	Growth constant for solidification of liquid region — Stage 3.
Λ_o	$\dfrac{C_B^{\beta o} - C_B^{\beta L}}{C_B^{\alpha L} - C_B^{\alpha o}}$
Λ_1	$\dfrac{C_B^{\alpha o} - C_B^{\alpha L}}{C_B^{\alpha L} - C_B^{\beta L}}$